Journal of Materials and Environmental Sciences
ISSN : 2028-2508
CODEN : JMESCN

J. Mater. Environ. Sci., 2018, Volume 9, Issue 2, Page 641-654

https://doi.org/10.26872/jmes.2018.9.2.71

http://www.jmaterenvironsci.com

Effect of Moist and Dry Heat Weathering Conditions on Cellulose Degradation of Historical Manuscripts exposed to Accelerated Ageing: ^{13}C NMR and FTIR Spectroscopy as a non-Invasive Monitoring Approach

B. Zghari[1], L. Hajji[1], A. Boukir[1*]

[1] *Laboratory of Applied Chemistry, Faculty of Sciences and Techniques of Fez, Sidi Mohammed Ben Abdellah University, BP 2202 – Route Imouzzer, Fez, Morocco.*

Received 22 Jun 2017,
Revised 21 Oct 2017,
Accepted 25 Oct 2017

Keywords,
- ✓ Archaeological Manuscript Paper,
- ✓ Cellulose Alteration,
- ✓ ^{13}C NMR CP-MAS,
- ✓ FTIR,
- ✓ Crystalline/Amorphous,
- ✓ Weathering Conditions, Ageing,
- ✓ Art Conservation Study.

aboukir@gmail.com;
Phone: +212 668 495 147

Abstract

Over time, paper undergoes unavoidable ageing process that results mainly in the degradation of cellulose. Paper endurance depends on its intrinsic properties, which are related to the environmental conditions and the manufacturing process. This work focused on evaluating the state of conservation of three restored ancient Moroccan manuscript papers (16th, 19th and 20th centuries) before and after artificial ageing over a period of 28 days at 90 °C and under two weathering conditions (dry-heat, moist-heat). In order to correctly discriminate samples, to inform on the conservation state as a preliminary step for the conservation process, and to elucidate well the structural changes in the chemical structure of cellulose polymers, a combined analytical approach has been applied for characterization, using solid state **^{13}C NMR-CP/MAS** and **FTIR** spectroscopy. The analysis was performed to carefully study the behavior of papers under extreme conditions of storage and to monitor artificial ageing effects. The IR crystalline phase is more dominant than the amorphous one (1475-1300 cm^{-1}), confirmed by ^{13}C NMR evaluation at C4 (88.7 ppm) and C6 (64.9 ppm). The phenomena of oxidation were shown after extended ageing 28 days in moist heat weathered conditions, and the cellulose alteration is more affected and pronounced in the 16th century samples. After ageing, the FTIR region (1800-1520 cm^{-1}) revealed the presence of oxidized groups corresponding to the C=O former. The cellulose degradation confirmed by the presence of intense and strong IR absorption bands of C=O at 1740 cm^{-1} (free –COOH; –COOR of normal and/or cyclic ester group: δ-valerolactone). Morever, the appearance of new polar, strong and relative intense IR bands at 1575 and 1539 cm^{-1} were attributed to C=O of carbonyls, originating from the contribution of oxidized low phenolic content in the lignin. The ^{13}C NMR signals with a weak and broad hump between 176-167 ppm justified the occurred oxidation and confirmed the deterioration process and the IR purpose.

1. Introduction

The chemical structure of the aged paper material is a complex mixture that is constituted by two dominant polymers cellulose and hemicelluloses; the lignins are absent or present at a very low percent. Cellulose polymer chains are the world's most abundant occurring, structured by several units of pyranose carbohydrates linked together by β-(1,4)-links and present a mixture of crystalline/ amorphous phase.

Where crystalline regions are alternate to amorphous ones, the polymer chains of cellulose are organized together in microfibril structure. Microfibrils are then aggregated into fibrils which in turn are aggregated into cellulose fibers [1-2]). Other fractions are present such as inorganic fillers, adhesives and sizing [3]. In cultural heritage material (ageing papers), the cellulose of material is exposed to many processes of degradation such as light, temperature, humidity, biological damages with a large number of microorganisms (fungi and bacteria) and partial hydrolysis [4], environmental conditions with reacting oxygen from the air or moisture, atmospheric deposition, leading to the alteration of its physical, chemical structure and mechanical properties, with a color change [5].

Deterioration of historical manuscript papers and artefacts stored in libraries and archives is responsible for an enormous loss of written cultural heritage. Consequently, restorers and conservators become more worried

about ancient book volumes that are in poor conditions. This interest concerns also the restored manuscripts that undergo degradation as a result of ageing. Therefore, understanding the degradation of paper is important for manuscript conservation purposes; especially for studying the long-term effect of a particular conservation-restoration treatment. Since natural paper ageing is too slow to permit the observation of structural changes in cellulose (oxidation, cristallinity index…) with a reasonable time frame, it is necessary to perform artificial or accelerated ageing methods [6-7].

Very few works with non-invasive techniques such as micro-raman have been applied to ancient manuscripts, especially to the typology of inks, dyes and pigments [8-9]. The art of conservation in cultural heritage concerns many areas, among which is the restoration of ageing archaeological materials, such as historical manuscripts papers. The nature of cellulose constituents plays a prominent role in determining the preservation state of historical papers. The IR spectroscopy as a non-invasive technique was used as an efficiency tools, for characterizing the cellulose structure, and informing on the state of archaeological material degradation by the occurred changes on the cristallinity and amorphous index, in order to conserve and preserve it [3,6,10-11].

Recently in 2015 and 2016, Hajji et al. [3,6,10], have been interest to historical Moroccan and Islamic manuscript papers, in order to assess their conservation and preservation with using SEM-EDS and XRD [3]. For the evaluation of the efficiency of the conservation-restoration treatment, a multi-analytical approach such as FTIR spectroscopy and solid state NMR spectroscopy have been used [10]. To assess a long-term of conservation treatment of ancient Moroccan manuscript papers, the combination of FTIR spectroscopy and energy dispersive X-ray fluorescence have been developed [6].

Modern Solid-state CP/MAS ^{13}C NMR technique is a non-invasive approach, useful to study a variety of interesting applications such as composite cellulose film [12], cellulose in archaeological woods [13], cellulose in archaeological ageing manuscripts papers [10], lignocellulose in wood tree [2], and lignocellulose in ageing Roman woods [14].

In this research work, a study of three restored Moroccan manuscript papers, dating to the 16th, 19th and 20th centuries, was carried out to evaluate the durability of Moroccan restoration processes and their efficacy in the preservation of written cultural heritage. Two accelerated ageing tests were carried out in controlled dry-heat (90 ± 2 °C) and moist-heat (90 ± 2 °C and 100% relative humidity) conditions. Among the various methods applied to study paper degradation, ATR-FTIR spectroscopy, solid state ^{13}C NMR/CP-MAS spectroscopy, have been used in this study in order to monitor the effects of artificial ageing in these particular conditions and are being compared with the results obtained after 28 days of exposure (dry and moist), to assess the state of cellulose degradation process evaluated by the variation in the spectra profile, and the degree of structural change between the crystalline and amorphous content in the altered cellulose.

2. Materials and methods

2.1. Sampling and Accelerated Ageing Methods

Samples were taken from three restored ancient Moroccan manuscript papers dating to the 16th (paper I), 19th (paper J) and 20th (paper H) centuries. These old documents belong to a private library located in the old medina of Fez (Figure 1).

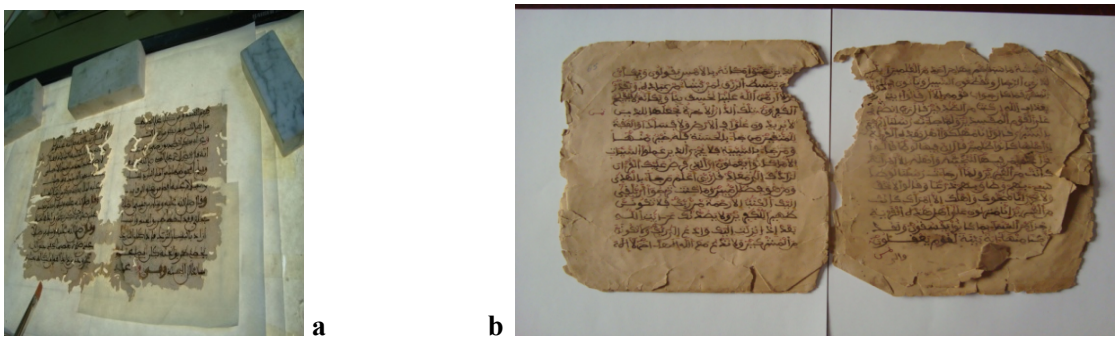

a **b**

Figure 1: An example of degraded Moroccan manuscript papers: (**a**: 19th centuries ; **b**: 20th centuries).

The dry heat weathering was applied by putting small piece of papers into sealed vials and introducing them into a controlled temperature dry heat oven at 90 ± 2 °C for 1, 3, 7, 21 and 28 days. While the moist heat weathering was performed by threading the paper sheets onto a cotton wire and suspending them a few centimeters above 1mL of distilled water in the sample vial. The vials were placed into a controlled temperature

dry heat oven at 90 ± 2 °C for 1, 3, 7, 21 and 28 days. Temperature and relative humidity in the vials should be 90 ± 2 °C and 100% relative humidity respectively.

2.2. Infra Red Spectroscopy (ATR-FTIR)

Spectra were obtained in the attenuated total reflection (ATR) mode using an infrared spectrometer (Brucker Vertex 70 model) equipped with a sampling accessory diamond window. The analyses were carried out at room temperature and ambient humidity. All the spectra were acquired between 4000 and 400 cm^{-1} with a spectral resolution of 4 cm^{-1} and 16 scans in order to exploit the instrumental built-up noise reduction algorithm. The spectra were collected in transmittance mode.

2.3. Solid State Nuclear Magnetic Resonance Spectroscopy (^{13}C NMR/CP-MAS)

Samples were finely cut and packed into 4 mm zirconia rotors and sealed with Kel-F caps. Solid-state ^{13}C CP-MAS NMR analyses were recorded on an NMR spectrometer (Bruker Avance 400 model) operating at 100.6 MHz ^{13}C NMR resonance frequency. Chemical shifts are given in parts per million (ppm). The spectrometer was equipped with a 4 mm Bruker MAS probe. ^{13}C CP-MAS NMR measurements were performed at room temperature with the following acquisition parameters: cross-polarization (CP) contact time 1 ms, repetition interval 3 s. The spin-rate was always kept at 12.5 kHz. NMR spectra were processed and analyzed with the TopSpin 2.1 software, as provided by the instrument manufacturer. Solid-state ^{13}C NMR was used as a non-destructive technique. All measurements were performed with no modification of the samples such as solvent extraction or other chemical treatment, making the samples available for further analytical investigation.

3. Results and Discussion

3.1. Dry-heat ageing Effects

3.1.1 FTIR analysis of dry heat aged samples

The ATR-FTIR spectrum of the analyzed sample dating to 20th centuries (H), is illustrated in Figure 2. The combined NMR ^{13}C data (Table 1) and FTIR spectra have been used to identify the constituents of historical papers; their detailed assignments are summarized in and Table 2. The IR fingerprint feature of cellulose is clearly encountered in all spectra; however, the difficulty is manifested in the more detailed interpretation of the IR chemical composition, due to the overlapping complexity of the different absorption signals of various constituents in historical papers. The area located between 1550-800 cm^{-1} is the most complex one of all the ranges, and the results for vibrations were consistent, informing well on the cellulose profile and characterizing the structural composition.

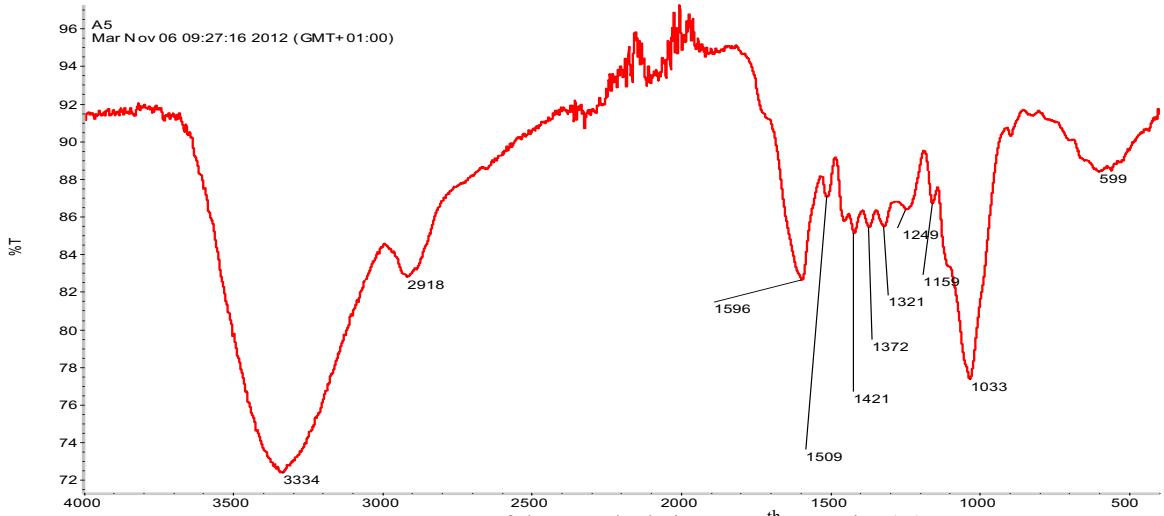

Figure 2: FTIR spectra of the sample dating to 20th centuries (H).

The fingerprint regions of the all spectra are rather similar as eleven out of the 14 discernable bands [15] are shared by the types of cellulose papers. In our studies, the characteristic profile of typical cellulose was detected in the regions of 3700-3100 cm^{-1} (νOH with two main vibrations: intra-molecular 3340 cm^{-1} and inter-molecular 3290 cm^{-1} hydrogen bonding in cellulose; νCH at 3000-2850 cm^{-1}, C-H bending: (*scissoring* and *wagging*; strong) at 1500-1300 cm^{-1}, the region between 1200-950 cm^{-1} corresponds to νC-O-C (strong and large with the very intense peak at 1025 cm^{-1}), and the β-(1,4)-glycosidic linkages in cellulose at 897 cm^{-1} attributed to νC_1-O-

C_4 (weak and broad) [16-18]. The main characteristic cellulose bands vibrations of our historical papers are: 3340, 3280, 2895, 1650, 1460, 1432, 1370, 1335, 1317, 1160, 1120, 1050, 1025, 897 cm^{-1}. Our results are in perfect agreement with the recent and various studies reported from 2015 to 2017 [4,15,18-19], who confirmed the presence of the same cellulose band absorptions in their archeological wood, spruce wood degraded, and transparent cellulose films respectively. While, Chen et al. 2016 [16] revealed the presence of cellulose wood bands at 1375, 1160, 1035 and 897 cm^{-1}, as well as the bands of hemicellulose near 1740 and 1240 cm^{-1}.

Monitoring aged samples by ATR-FTIR spectroscopy allowed us to study the structural changes of cellulose feature due to thermal degradation of papers. It was found out that the exposure to a high temperature for an extended duration caused profound changes in the OH bonds network in the cellulose, considering that the intensity of the band related to OH stretching (3100-3600 cm^{-1}) [10,20] has significantly decreased after 21 and 28 days of treatment. The variability was very pronounced on the large absorbance band at 1200-950 cm^{-1}; however, the lowest variation was found in band at 897 cm^{-1}. The slight variation corresponds to the peaks at 897, 1335, 1370, 1460, 1534, 1579 cm^{-1}; while the bands at 1317, 1432, 1650 cm^{-1}, and the largest signal between 1200-950 cm^{-1} (1160, 1120, 1050, 1025 cm^{-1}), presented an extremely large variation. In addition, the ageing process promoted the breakage of the C-O-C bonds in the β-(1,4)-glycosidic linkage (897 cm^{-1}) of crystalline cellulose [10,16-18,21] and in pyran sugar (1105-1000 cm^{-1}) considered as the most sensitive to ageing and thermal perturbation [16].

The dry-heat ageing phenomenon presents no effect during the treatment phases, and it might be explained by the absence of oxidized former functions (carbonyl groups) discerned at 1710-1740 cm^{-1}, so we could suggest that no generation of cellulose oxidation in the restored paper studied.

IR crystalline cellulose

The crystalline cellulose form (*strong* band) absorbs at 1425 cm^{-1}, and corresponds to CH_2 symmetric bending in *crystallized* cellulose I [17-18]. Its empirical crystallinity index has been reported with a ratio of the peaks at I_{1427}/I_{897} [17-18]. While the *amorphous* cellulose form (*weak* peak) shift to 1420 cm^{-1} in cellulose II [22]. According to Abidi et al. 2014 [17], the C-H in plane bending signal at 1375 cm^{-1} is the most appropriate for indicating cellulose *crystallinity* in ratio with the peak at 2900 cm^{-1} (I_{1375}/I_{2900}). Referring to recent literature report, Hajji et al. (2015) [10], have assigned the band absorption at 1317 cm^{-1} to C-H bending vibration in *crystallized* cellulose form, while the C-H bending vibration of *amorphous* cellulose form arised as a *shoulder* at 1330 cm^{-1}.

The cellulose contents (*crystalline* and *amorphous*) are less sensitive to the effect of dry-heat ageing with predominance of the *crystalline* phase than the *amorphous* one.

Inorganic filler

The inorganic filler of $CaCO_3$ was investigated and identified by the *broad* stretching asymmetric absorption peak at 1425 cm^{-1} (ν_{as}C-O in CO_3^{2-}), and two *weak* peaks at 874 (stretching symmetric ν_sC-O of $CaCO_3$) and 710 cm^{-1} (in plane deformation δ(OCO) in CO_3^{2-} groups of $CaCO_3$). The presence of IR inorganic filler results were confirmed also in recent works by Hajji et al., 2015 [3,10] with using XRD analysis. Referring to their published studies, the kaolin was identified as an inorganic filler and showed the characteristic bands near 3750-3660 (νAl-OH), 3735 (νSi-OH), 1040 (ν_{as}Si-O-Si), 1000 (Si-O-Al link and Si-O-Si), 1000-950 (Al-O), 524 (angular deformation Si-O-Al link), 466 cm^{-1} (angular deformation Si-O-Si). So, in our case study, we confirmed the presence of kaolin by the high frequencies absorption bands overlapping with the cellulose bands (O-H, C-O) as reported by Hajji et al., 2015 [3] and by the low frequencies signals at 560 and 430 cm^{-1}.

3.1.2 Solid-Stae ^{13}C NMR CP-MAS analysis of dry-heat aged samples

The monomeric structure unit of cellulose (pyran sugar) is illustrated in Figure 3, and the ^{13}C NMR CP/MAS spectrum of the sample datin to 19th centuries is shown in Figure 4.

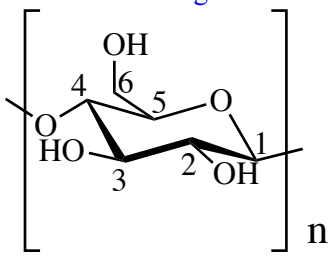

Figure 3: Monomeric pyran carbohydrate structure unit of cellulose

The ^{13}C NMR profile of cellulose is clearly manifested in all spectra (Figure 4), with board resonances that extend over chemical shift ranges of 61 to 107 ppm, showing an appreciable variation in the intensities of the solid matrix of papers and permitting to distinguish between the *crystalline* and *amorphous* phase in the cellulose content (Table 1). Solid-state ^{13}C NMR as a non-destructive technique, was used to obtain information on the conservation state of the manuscripts papers as a preliminary step for the conservation process, then to assess the occurrence of alteration of the manuscript papers under dry-heat artificial ageing, and finally, to evaluate the produced change on the predominance degree of crystalline or amorphous phase in the cellulose content, after ageing conditions [2,10,13-14,20-21,23-25].

The main intense overlapping signals ascribed to C_2, C_3, C_5 exhibit variable absorption positions, and resonate between 71-75 ppm. The deshielded signal located at 103-107 ppm was attributed to anomeric carbon C_1 (ketal function) of cellulose I_β and I_α, while the carbon C_6 resonates at low frequencies between 61-65 ppm. The C_4 responsible on the β-1,4-glycosidic linkages in cellulose is shifted to low field and resonates between 84-89 ppm. The presence of the major crystalline form with respect to the amorphous one, was manifested by the high-intensity signals at the C_4 (88.7 ppm) and C_6 (64.9 ppm), while the amorphous form is demonstrated by a broad and low-intensity signals centered at (84 ppm, C_4) and (62 ppm, C_6). Basing on the Bastone S. et al. 2016 [14] and M. Foston [25] studies, the allomorphs cellulose (I_α and I_β) are considered such as the two naturally occurring crystalline cellulose polymorphs.

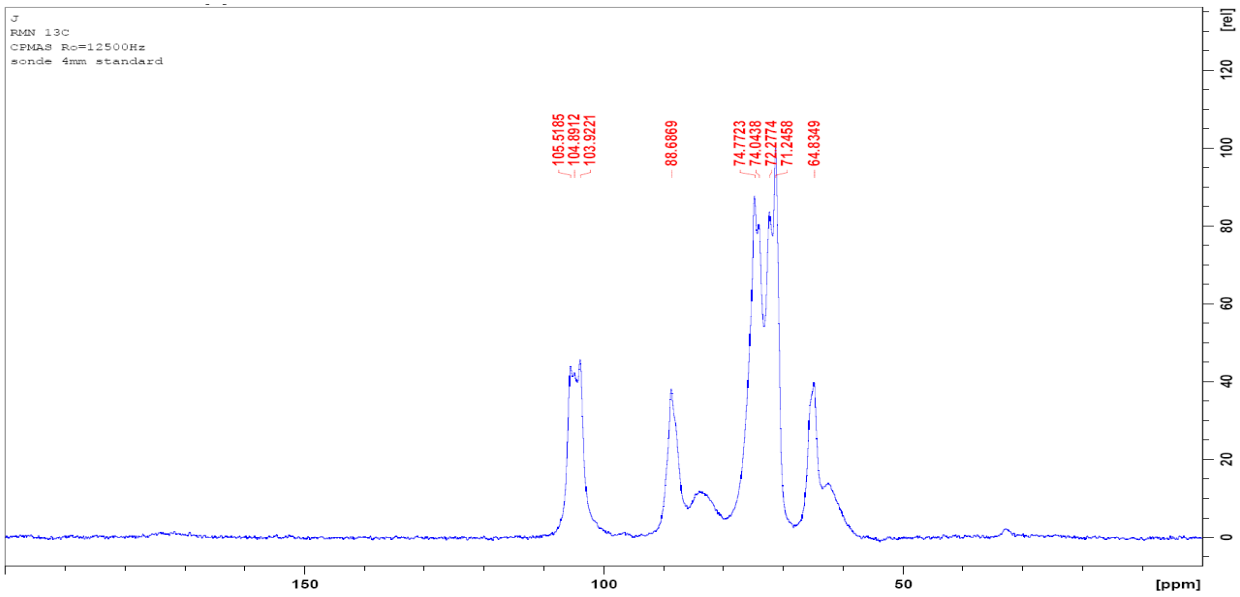

Figure 4: ^{13}C NMR CP-MAS spectra of the cultural heritage manuscript samples (19th centuries (J): dry-heat conditions 90 °C; 28 days of ageing).

In the ^{13}C NMR spectrum data (19th centuries (J), Figure 4), the absence of the signal more than 167 ppm, dismisses the presence of the degraded form of cellulose. So, the obtained NMR results agree well with those of our IR finding. In recent works from 2015 and 2017, some authors [12,26] have attributed the chemical shift between 160-170 ppm to the C=O of acetoxy group (–COO-CH_3) in 8 different acetyl-monomers of cellulose acetate derivatives.

According to several past XRD works [4,6,10,18,27-29], the X-ray diffraction patterns show four crystalline characteristic major peaks of native cellulose (cellulose I) at 14.5°, 16.5°, 22.6° and 34.5° 2θ intensity, which are ascribed to ($1\bar{1}0$), (110), (200) and (040) crystallographic planes, respectively; while for the amorphous phase, diffracted profile is described at 18.5° 2θ intensity. The results showed that important crystal phase change of native cellulose occurred during the artificial ageing, especially for a prolonged time of treatment (21 and 28 days). This is explained by the strong decrease in the intensity of the diffraction peaks ($1\bar{1}0$), (110) and (200) characteristic of native cellulose [3,30].

Based on published XRD works concerning the deterioration of manuscript papers [6], our ^{13}C NMR crystalline phase stills presenting the most accentuated degree than the amorphous one, after thermal (dry-heat) and ageing alteration (28 days).

Table 1: ^{13}C NMR CP-MAS chemical shift and assignments of the historical manuscript samples after 28 days of ageing (19th centuries (J): dry-heat 90 °C, Figure 4; and 16th centuries (I): moist-heat conditions 90 °C, Figure 6 and 7 (NMR 4 spectrum)). [2,10,13-14,23,25-26].

Carbon number	^{13}C NMR **assignment, δ (ppm)** (19th (J): dry-heat 90 °C, 28 days of ageing; Figure 4)	^{13}C NMR **assignment, δ (ppm)** (16th (I): moist-heat 90 °C, 28 days of ageing; Figure 6 and 7 (NMR 4 spectrum)
C_1 (anomeric)	106.69 (cellulose I_β of anomeric carbon) 104.93 (cellulose I_α of anomeric carbon) 103.99 (cellulose I_β of anomeric carbon)	105.578 (cellulose I_β of anomeric carbon) 104.809 (cellulose I_α of anomeric carbon) 103.904 (cellulose I_β of anomeric carbon)
C_4	88.77 (crystalline form of β-1,4 glycosidic linkages in cellulose with predominant degree) 84.23 (amorphous form of β-1,4 glycosidic linkage in cellulose with minor degree)	88.71 (crystalline form of β-1,4 glycosidic linkages in cellulose with predominant degree) 83.93 (amorphous form of β-1,4 glycosidic linkages in cellulose with minor degree)
$C_{2,3,5}$	74.826, 74.820, 74.069, 72.331, 71.289 (overlapping signals)	74.794, 74.036, 72.314, 71.253 (overlapping signals)
C_6	64.876 (crystalline form with predominant degree), 61.953 (amorphous form with minor degree)	64.884 (crystalline form with predominant degree), 62. 50 (amorphous form with minor degree)
C=O	-	176-170 carbonyl of degraded cellulose: –COOR (ester, δ-valerolactone), and –COOH

3.2. Moist heat ageing Effects

The second approach was to subject the restored manuscript papers to extreme conditions in a moist heat environment at a temperature of 90 ± 2 °C and 100% of relative humidity.

3.2.1 FTIR analysis of moist-heat aged samples

The FTIR superposition spectra of the untreated and treated moist heat ageing weathered paper I (16th centuries) for 1, 3, 7, 21 and 28 days, are exhibited in figure **5**; and showed all the characteristic absorption bands of polysaccharides (Table 2). Concerning the assessment of the weathering effect with moist heat ageing (% relative humidity), the FTIR spectra profile showed that a serious evolution of cellulose degradation occurred during artificial ageing with moist-heat conditions, and especially for an extended time span of treatment for the aged 16th centuries sample (21 and 28 days), followed by the aged 3-day and aged 7-day samples (Figure 5). The most sensitive to deterioration and affected one was the 16th centuries sample, with appearance of very marked oxidized bands, after 28 days of accelerated ageing process (Figure 5, aged for 28 days).

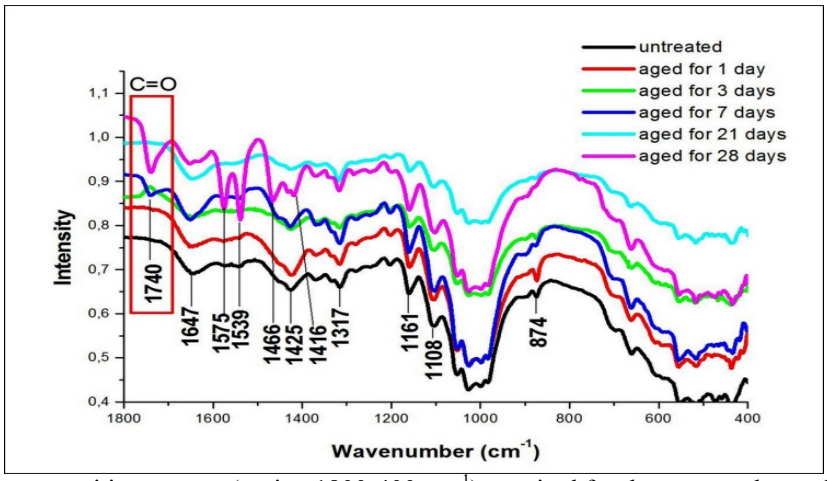

Figure 5: ATR-FTIR superposition spectra (region 1800-400 cm^{-1}) acquired for the untreated sample (16th centuries (I: reference)) and after ageing in moist-heat conditions 90 °C, during 1, 3, 7 , 21 and 28 days [6].

The main specific chemical changes concerned the decreasing in the bands related to associated hydrogen-bond stretching vibrations of OH group in alcohols (3700-3100 cm^{-1}), bending O-H of adsorbed water (1647 cm^{-}

[1]) [10] and O-H out of plane bending (800-400 cm^{-1}); C-H stretching vibrations (3000-2850 cm^{-1}) and C-H in plane bending 1425 cm^{-1} (H-C-H, O-C-H) [22]. Drastic changes and decreasing of the broad intensities absorptions and shape of the largest bands (dominant fingerprint feature of cellulosic region) have been shown in the wide range of 1200-850 cm^{-1}; indicating that the cellulose alteration occurred on the C-O-C bridge bond of carbohydrates in cellulose (1161 cm^{-1}), C_{alk}-O-C of skeletal vibration of polysaccharides ring (1030 cm^{-1}, pyranose), affecting the C_1-O-C_4 β-(1,4)-glycosidic linkages (897 cm^{-1}) between pyranose sugar units of cellulose [4,6,17] and finally the disappearance of the band at 874 cm^{-1}.

Table 2: FTIR data of cellulose content in Moroccan historical manuscript samples exposed to accelerated ageing (1 to 28 days; in dry and moist weathering conditions) [3-6,10,15-19,22,31-36].

Wavenumber (cm^{-1})	**Band assignments**
3700-3100	νOH: stretching vibration of O–H groups in cellulose and hemicellulose (*broad band*) with two main vibrations (3340 cm^{-1}, 3290 cm^{-1}); and νOH of absorbed water [10,17]: *intra*-molecular (3340 cm^{-1}) and *inter*-molecular hydrogen bonding (3290 cm^{-1}) [17,18]
2923-2853	$\nu_{as}CH_2$ and ν_sCH_2 in methylene [33,34]
2909-2896	νC–H in methylidene [33,34]
1740	νC=O stretching vibration of carbonyl group of normal ester, acetoxy group H_3C–(C=O)–O– in hemicellulose; and/or cyclic ester (such as γ-lactone [32], and/or C=O of free carboxyl acid group [36]
1647	δ O–H in plane bending vibration of adsorbed water (*broad* and *strong*) [3,6,10;17], and/or νC=O carbonyl group in resin: 1658 cm^{-1} [4,16]
1575	νC=O stretch in skeletal vibration of phenolic ring [16,33]as a contribution of lignin [4]
1539	νC=O stretch in skeletal vibration of phenolic as a contribution of lignin [16]
1470-1472	δCH_2 *asym* [36]: strong in cellulose I (in *crystalline* phase CH_2) [35]
1466-1462	δCH_2 *sym*: in plane bending (*scissoring*) [33-34] strong in cellulose I (in *crystalline* phase CH_2 and *asym* in *amorphous* CH_2) [35] δCH_3 *asym* bending in lignin (CH_3–O) and hemicelluloses (CH_3–(C=O)–)
1445	O–H in plane deformation (*shoulder*) [17]
1430	Characteristic of cellulose I with the band at 1108 cm^{-1} (sign of cristalline form) [5] H–C–H and O–C–H in plane bending vibrations [22] V_{as}C–O in CO_3^{2-} groups of $CaCO_3$ as a contribution of calcite (inorganic filler) and δ_sCH_2 at C6 of celluose [3]
1425	δCH_2 symmetric bending in *crystallized* cellulose I (*strong*); [17] and *amorphous* cellulose (*weak* and shift to 1420 cm^{-1} in cellulose II and *amorphous* cellulose) [22], and/or ν_{as}C–O in CO_3^{2-} of $CaCO_3$ inorganic filler, with a *broad* band [10]
1416	CH_2 (*scissoring*), *amorphous* cellulose shift to 1416 cm^{-1} in cellulose II (*crystalline*)),
1375	C–H deformation vibrations in cellulose [22], (most suitable for indicating cellulose *crystallinity* in ratio with 2900 cm^{-1} vibration) [5,17]
1372, 1335 and 1316	3 typical bands of *crystalline* cellulose [5]
1330	C–H bending vibration in *amorphous* cellulose (*shoulder*) [10] *crystalline* cellulose [5]
1317	C–H bending vibration in *crystallized* cellulose I [5,10] (CH_2 *wagging* or CH_2 rocking [31])
1280	Typical band of crystalline cellulose [5]
1268	νC–O stretching vibration of carboxyl group [16];
1230	νC–O stretching vibration of carbonyl ester group in hemicellulose [16]
1161	νC–O–C *asym* bridge stretching vibration in cellulose [4,19]
1108	Characteristic of cellulose I with the band at 1430 cm^{-1} (sign of cristalline form) [5] νC–O *asym* in plane vibration valence of pyranose ring of polysaccharides [19] CH stretching vibrations in different groups of carbohydrates

1000-900	many signals of cellulose vibrations modes
1053	νC–O bond of aliphatic **C**–**O**H vibration [4]
1030	νC_{alk}–O–C stretching mode of skeletal vibration of polysaccharides (pyranose ring) [4,36]
995	νC–O valence vibration [4]
897	νC_1–O–C β-(1,4)-glycosidic linkages between glucose units in cellulose (*weak* and *broad* in cellulose I (amorphous) [5,22]; *strong* and *sharp* in cellulose II (crystalline) [4,5,17,18,22]
874	ν_sC–O of $CaCO_3$ as a contribution of calcite (inorganic filler) [3,10]
710	r$(CH_2)_n$ (n>4) rocking in *crystalline* cellulose I_β as a shoulder; [17,33,34] ; and/or δ (OCO) in CO_3^{2-} groups (in plane deformation) of $CaCO_3$, [3,10]
667	δ_{oop}O–H out of plane bending vibration (700-400 cm^{-1}) of alcohol groups in cellulose, hemicellulose and/or OH of carboxylic acid
560	δ (Si–O) in kaolin (inorganic filler) [3,10]
430	δ (Al–O–Si) in kaolin (inorganic filler) [3,10]

As shown in literature reports, the evolution of the sharp and intense band at 897 cm^{-1} of crystalline form [17-18] towards the broad and weak signal (amorphous form) [5], reflects higher disorder in structure [37-38], manifesting the formation of a larger amount of amorphous phase [5,39]. As reported by recent work of Chen et al. 2016 [16], the signal at 897 cm^{-1} is the most sensitive to the thermal perturbation. Based on literature data [5,16,17-18,37-39], in our case studies the evolution of the absorption band at 897 cm^{-1} towards a broad and weak one after 7 to 28 days of moist-heat ageing, is a sign of the presence of a dominant amount of amorphous form. The impact of extended ageing (21-28 days of exposure), thermal perturbation and moist effect leads to the marked and sensitive broadening former band instead of 874 cm^{-1}, promoting the destruction of the β-(1,4)-glycosidic linkages, reflecting higher disorder in structure, and favoring the monomer former units of carbohydrates; recombining and reorganizing itself in another structure form (amorphous structure) [5].

The marked decrease of the sharp intensity bands of the inorganic filler at 874 cm^{-1} (ν_sC–O of $CaCO_3$) until disappearance (after 7th day of exposure, under moist-dry heat) is a sign of the absence of calcite ($CaCO_3$) reflecting its sensitivity to the expressed weathering conditions, especially to humidity and prolonged ageing process effect from 21 to 28 days. Referring to EDXRF studies reported by Hajji et al. 2016 [6], they confirmed the presence of Ca with a slight decrease in their content after 28 days of ageing.

3.2.1.1 IR region 1800-1500 cm^{-1} and NMR analysis

The cellulose degradation phenomenon is more pronounced and profoundly marked in the 16 centuries sample (I) after 28 days of extended moist-ageing effect, firstly, by the appearance and increasing of a new absorption signals between 1800-1500 cm^{-1}; and secondly, by the occurred changes on the ratio of crystalline/amorphous content in the area of 1500-1100 cm^{-1}. The appearance of 3 new intense and polar bands with extended ageing are ascribable to the carbonyl groups (1740, 1575 and 1539 cm^{-1}) but not clearly elucidated yet by literature data (Figure 5, aged for 28 days), and they testified to the occurrence of oxidative process [6,40].

In fact, the examination of FTIR spectra related to all samples revealed that the new arising absorption signal at 1740 cm^{-1} mainly in the aged one (16th centuries (I)) and after 28 days of ageing (Figure 5) is assigned to normal carbonyl ester group [14-16,39] or to cyclic ester group such as δ-valerolactone, [6,32,41-42]; which indicates the increasing of C=O content and confirmed the occurrence of deterioration process. As known, the presence of the carboxyl acid group could be explained by the occurrence of oxidative reaction of cyclic *gem*-diol or external CH_2OH in pyran ring of cellulose; leading after oxidative reaction to the formation of carbonyl aldehydic groups (-CH=O), which react in more oxidative forms such as carboxyl acid groups (-CO_2H) and permit to explain the alteration mechanism during the ageing process. A part of formed carboxylic acids, could react and recombine with the alcohols via an *internal* and/or *external* molecular esterification reaction giving arise to the formation of new C=O absorption bands of ester groups. Thus, the presence of the signal at 1740 cm^{-1} might be assigned to the carbonyl groups of ester groups (normal and/or cyclic such as δ-valerolactone) and C=O of unreacted carboxylic acid groups; this purpose was confirmed by the ^{13}C NMR spectra in the area of 167-176 ppm. Referring to literature studies [6,31-34], the absorption band at 1740 cm^{-1} was ascribed also to the free carbonyl group of carboxyl acid group.

Concerning the band centered at 1647 cm^{-1} and according to literature data, this absorption is related to the δ(OH) bending of adsorbed water, and appears generally between 1635-1647 cm^{-1} [3,4,10]. The decrease in this

broad signal between 1620-1650 cm^{-1} provides information on the alteration or weakening of the hydrogen-bonded cellulosic chains (*intra* and *inter*molecular) and promotes the degradation phenomenon.

The two new and intense remaining marked bands appearing at 1575 [4,31,42] and 1539 cm^{-1} (Figure 5, aged for 28 days) are correlated to C=O stretching vibration of carbonyl groups. The complexity of assignment is manifested by the overlapped absorption with various signals in a very narrow area. So, the manifested polar character of the new arising peak at 1539 cm^{-1} exhibited by a strong absorption leaves no doubt on its attribution to the C=O group, justified also by its absence in the 5 others IR spectra samples of untreated (reference) and treated ones (1, 3, 7, 21 days) (Figure 5). In recent works, Tamburini et al. 2017 [4] have ascribed the presence of the strong band at 1593 cm^{-1} to the C=O group, and its increase is correlated to an effect of the lignin content. According to Chen et al. studies [16] the absorption peak at 1588 cm^{-1} is correlated to the presence of C=O group in Benzoinum wood resins (associated with other peaks at 1732, 1695, 1666 and 1523 cm^{-1}), which are the most sensitive to thermal perturbation [16]. Recently, Hajji et al. 2016 [6] have linked the band at 1620 cm^{-1} to C=O group of diconjugate aromatic ketones (Ar-CO-Ar), but we did not agree to this attribution, because in our case, the chemical shift of aromatic ring can be ruled out by the absence of their ^{13}C NMR signals between 105-160 ppm (Figure 4, 6 and 7). Generally, and as known, the IR bands at 1620-1600 and 1500 cm^{-1} are related to aromatic C=C and appear with fine and sharp absorption peaks. Hajji et al. 2015 [3] and cited references in, have correlated the signal at 1542 cm^{-1} to the N-H in plane bending vibration, which could originate from protein [3,17] of animal, and used as adhesive glue in paper content. In our case, this attribution could be discarded, because we note the absence of this band in the both original spectrum (untreated) and treated spectra dating from 1, 3, 7, 21 days.

As shown, by FTIR (Figure 5, aged 28 days) the IR C=O absorption at 1740 cm^{-1} (ester and/or carboxylic acid groups) is confirmed by ^{13}C NMR spectra in the range of 167-176 ppm (Figure 7 and 8), and considered as a result of the degradation process of cellulose. Concerning the two strong and polar bands at 1575 and 1539 cm^{-1} could be attributed to C=O of carbonyl groups and might be explained by the contribution of a very low relative amount of oxidized phenolic lignins influenced by the effect of temperature, humidity, and extended ageing time (28 days). So, this finding proves that the cellulose constituents of 28-day aged sample of 16 centuries (I) are more affected than the lignin with low rate of contribution and more sensitive to both temperature [16] moist and ageing effects.

With using ^{13}C NMR/CP-MAS, a broad and weak signal as a hump was detected and displayed between 167-176 ppm in the spectra (28-day aged) of weathered papers (Figure 7 and 8) revealing the occurrence of oxidative reactions, and is mainly ascribable to carboxyl acid group [10,24]. The NMR results corroborate well with obtained FTIR data and reveal the occurrence of degradation process with promotion towards free saturated carboxyl acid group ($-CO_2H$) justified by the presence of C=O (167-176 ppm) with absence of conjugate form $C=C-CO_2H$ (no NMR signals of C=C between 100-150 ppm) (Figure 4, 6 and 7).

Kono et al. (2017) [26] and Paci et al. 1995 [24] assigned the chemical shift between 168-170 ppm to carbonyl group of ester (acetyl group) [12,26], while the attribution of this signal stills subject of many controversies in the literature reports [10,24,26]. So, in our case study, the combination of NMR and IR spectroscopy data provide information on the presence of carbonyl group of normal and/or cyclic ester (such as δ-valerolactone). This finding is confirmed by the presence of a strong infrared absorption band at 1740 cm^{-1} [31] and NMR weak hump resonating at around 170-176 ppm (Figure 7 and 8) elucidating well their presence; so, the obtained result can't be ruled out. As for the C=O group of carboxyl acid, its presence is not to be dismissed, resonating at the same range of carbonyl ester group and revealed by the NMR hump with weak signal at 170-176 ppm (Figure 7) and 167-176 ppm (Figure 8).

3.2.1.2 IR region 1500-1110 cm^{-1} of moist-heat aged samples and crystalline form Crystallinity index

The appearance of new peaks after moist-heat ageing demonstrates the produced changes in the reorganization of the polymer chain [10,40]. The main change in this region has been evident in the crystalline and amorphous phases in the range of 1500-1300 cm^{-1} after 28 days of thermal and ageing process. The crystalline form of cellulose I, in all IR spectra of Moroccan manuscript papers samples (16^{th}, 19^{th} and 20^{h} centuries) was confirmed by the presence of strong absorption band at 1425 cm^{-1} [17] and the absence of the amorphous form at 1420 cm^{-1}. However, we note that in the 16^{th} centuries IR spectrum and after 28 days of ageing, the arising of absorption signal shifted towards 1416 cm^{-1} and revealed the existence of amorphous structure. The presence of both IR crystalline/amorphous content in our samples agree well with those of the X-ray obtained by Hajji et al. in 2016 [6] on the ancient manuscripts papers (16^{th} and 18^{th} centuries).

3.2.1.3 16th century samples after 1 to 28 days of ageing

Except for the 28-day aged sample spectrum; all sample spectra (untreated, and treated from 1 to 21 days) (Figure 5) have four more abundant bands at 1500-1400 cm^{-1} (shape of the board signal), 1317, 1161 cm^{-1}, followed by the slightly less intense band at 1375 cm^{-1} and are all relative to the degraded cellulose. The broad signal between 1500 and 1400 cm^{-1} contains a mixture of two unresolved crystalline and amorphous phases. Thus, the sample treated during 28 days presents a peculiarity by the appearance of 3 new signals well resolved at 1466, 1425 and 1416 cm^{-1}. The first is the most abundant one, containing the mixture of two unresolved forms (crystalline and amorphous), followed by the peak at 1416 cm^{-1} corresponding to the resolved amorphous form, while the least intense peak at 1425 cm^{-1} is attributed to the resolved crystalline form [17-18].

So, our IR spectrum results (28 days aged) confirmed that the crystalline phase content is the major constituent (cellulose I) with the following absorptions signals at 1425, 1375, 1317 cm^{-1} [17-18] and 1335 cm^{-1}, more than the amorphous one (cellulose II) with the presence of only one resolved peak at 1416 cm^{-1} and absence of the band at 1330 cm^{-1}. As reported by Hajji et al. (2015, 2016) ([3,6,10] and Colom et al. 2002 [44]; the presence of two broad bands as a doublet at 1335 and 1317 cm^{-1} is ascribed to the mixture contents of crystallized and amorphous cellulose forms, respectively. While Abidi et al. (2014, 2017) [17-18]) have correlated the only band at 1315 cm^{-1} to the crystalline form. The peculiarity of the presence and evolution of the doublet bands at 1335 (sensitive and disappears in biodegradation) and 1317 cm^{-1} (most intense) provide information on the occurred cellulose alteration, and/or on the presence of higher cellulose I content; this finding is reported by Oldak et al. 2005 [45]. The ratio of this doublet (I_{1317}/I_{1335}) was used to monitor the degree of alteration and to specify that the amorphous form is the most sensitive to degradation than the crystalline one [45].

The calculation of IR crystallinity index is subject to several controversies with referring to various recent studies and author's reports [5,10,17-18,22,35,44]. Hajji et al. 2015 [10] showed that the information on the higher content of crystalline or amorphous fraction could be obtained by the ratio of the doublet of peaks at 1315 cm^{-1} (crystallized form) and 1330 cm^{-1} (amorphous form) I_{1315}/I_{1330} ; while Song et al. (2015) [22] used the ratio of the signals at I_{1430}/I_{900} due to the sensitivity of those bands in order to characterize the structure of cellulose I. In recent works, and in order to determine the empirical crystallinity index, Abidi et al. (2014 and 2017) [17-18]) have used the ratio of the bands at I_{1427}/I_{897} .

The unresolved broad band at 1500-1400 cm^{-1} is a good indicator on the presence of a mixture of crystalline and amorphous content [35]. The reduction shown in the intensities of the two resolved signals (IR spectrum 28-day aged) at 1425 (characteristic of cellulose I) and 1108 cm^{-1}, reflecting the absence of the crystalline cellulose I degree. This finding is supported by previous studies [5,44]. In our case study, the decreasing of the intensities of the specific carbohydrate bands (897, 1416, 1425, 1466 cm^{-1}) and the enhancement of the signal at 1738 cm^{-1} is an alteration indicator, due to the impact of both aged exposition and weathering effect of temperature. According to, kavkler el al. (2011) [5], the decreasing absorptions signals at 1375, 1160, 897 cm^{-1} were correlated to the cellulose deterioration under fungal effect, and therefore agree with part of our results corresponding to cellulose alteration under moist-ageing effects.

3.2.2 Solid-State ^{13}C NMR CP-MAS analysis of moist heat aged samples

The ^{13}C NMR as a nondestructively tools was used in order to assess and to discriminate the state and the degrees of moist-heat and the effect of ageing (1, 3, 7, 21, 28 days) on historical documents deterioration dating to 16th centuries. Figure 7, shows the superposition ^{13}C NMR spectra of 5 samples (NMR 1-5) corresponding to accelerated ageing during 1, 3, 7, 28 and 21 days, respectively.

Compared to the ^{13}C NMR spectra under thermal effect, no profound shift has been effected in the chemical shifts of 2 moist-aged cellulose samples (19th and 20th centuries) and the feature is still quite similar, except for the 16 centuries sample after treatment for 1, 3, 7, 21 and 28 days of ageing under moist-heat weathering conditions (Figure 6, 7 and Table 1). The pronounced alteration has been manifested and very marked in the sample NMR 4 after 28 days of ageing and elucidated by ^{13}C NMR (Figure 6, 7).

However, the induced change has been evident by the enhancement in signal intensities at C_1 of cellulose I_α and I_β (103.9-105.6 ppm), C_4 (83.9-88.7-ppm), C_6 (62.5-64.9ppm), and C_2 , C_3 , C_5 (71.3-74.8 ppm), favouring the formation of the crystalline form. Thus, the crystalline forms increase from the 3rd to the 28st days of ageing, manifested on the allomorphs Iα and Iβ of C_1; on the deshielded peak of C_4, shielded signal of C_6, and on the large absorptions of C_2 , C_3 , C_5 (71.3-74.8 ppm). The result is that the increasing crystallinity and amorphous degree were very marked mainly at the 28th days of ageing, followed by the 21th and 7th days at the same level. As for the crystalline phase, it remains more predominant compared to that of amorphous in all signals.

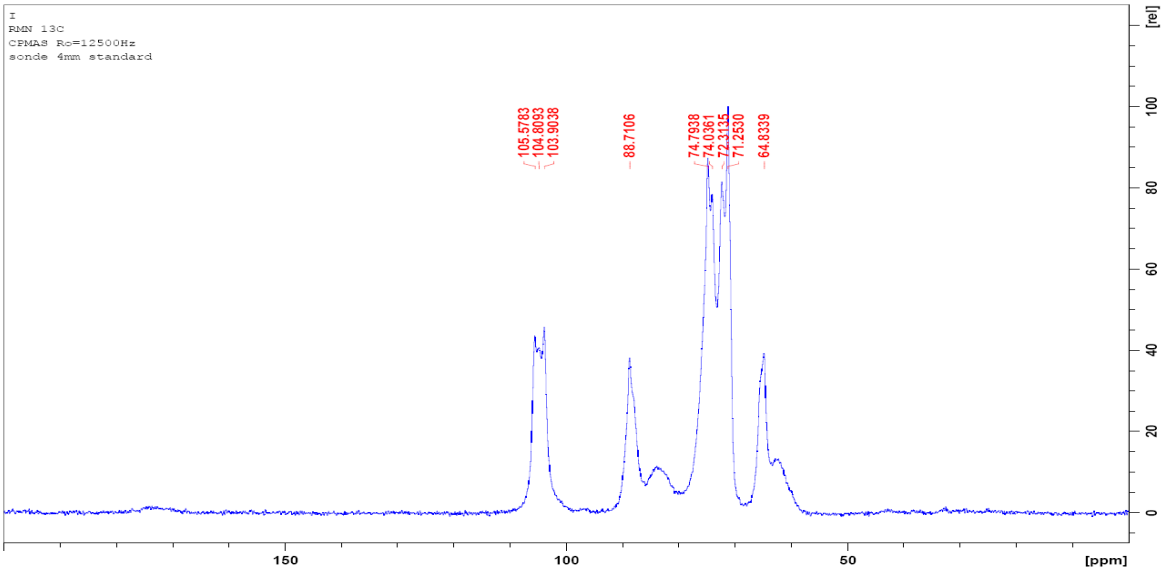

Figure 6:[13]C NMR CP-MAS spectra of the cultural heritage manuscript samples (16th centuries (I): moist-heat conditions 90 °C with ageing for 28 days) [10].

The oxidation of the cellulose was observed after 28 days of ageing process, proved by the appearance of the very broad signal in the form of a hump with a very low intensity between 167-176 ppm. Thus, the shift between 170-176 ppm confirmed its degradation and deterioration by arising of a new C=O of ester groups (normal ester, cyclic ester δ-valerolactone) and new C=O of carboxylic acid group derivating from ester hydrolysis reaction. The presence of water resulting from 28 days of ageing (confirmed by IR at 1650 cm^{-1} as adsorbed water [3-10]) facilitates the hydrolysis reaction of ester submitted to an acid-catalyzed by cellulose hydroxyl groups, and then, the dissociation of the cellulose hydroxyl groups (–COOR) to carboxylic acid group (–COOH) is occurred in the current reaction [26]. Morever, the arising signal (weak and broad) between 167-176 ppm (Figure 7 and 8 (NMR 4)) reflects the presence of recombined C=O of ester group such as acetyl substituent distribution as a results of degradation processes [26], probably located on selected positions of cellulose hydroxyl groups carbons C_1 to C_3 **and** C_5 **to** C_6 with decreasing in their chemical shifts as $C_6 \gg C_3 > C_2$, as reported in recent studies by Kono et al. (2017) [26].

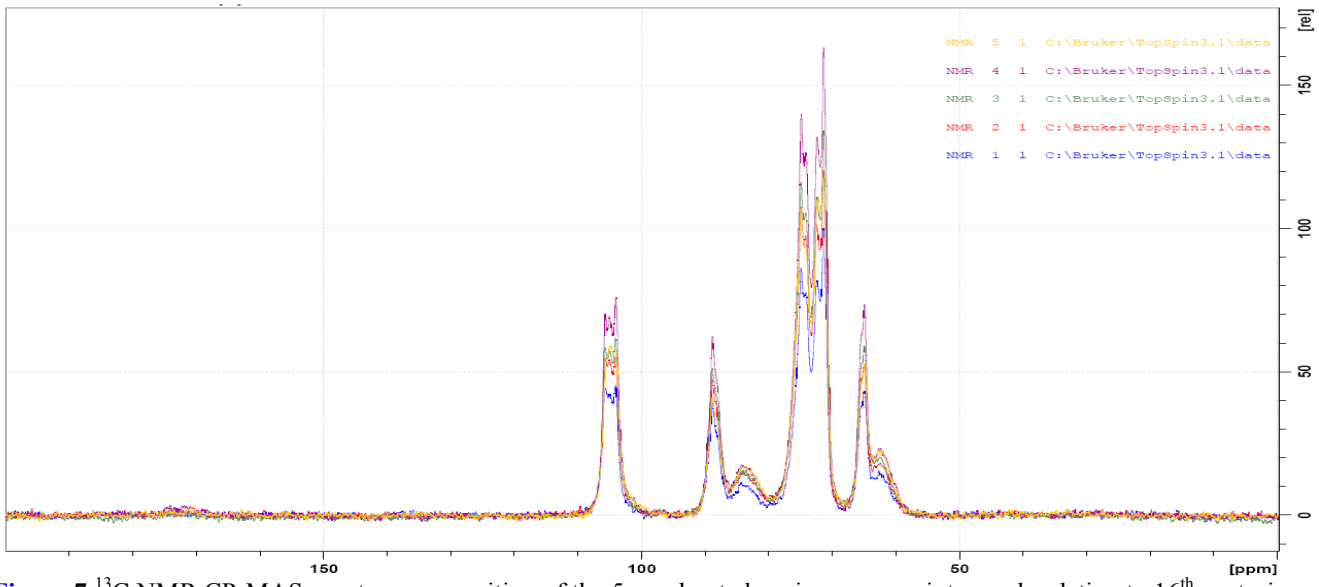

Figure 7:[13]C NMR CP-MAS spectra superposition of the 5 accelerated ageing manuscript samples dating to 16th centuries, under moist-heat conditions 90 °C (**NMR 1**: 1 day, **NMR 2**: 3 days, **NMR 3**: 7 days, **NMR 5**: 21 days, **NMR 4**: 28 days).

The [13]C NMR results obtained from the 16th centuries sample (NMR 4: moist-heat and 28 days of ageing) are in complete agreement with our IR finding and illustrated well the cellulose deterioration (167-176 ppm) justifying the presence of many types of C=O groups ascribable to ester groups, carboxylic acid and carbonyls

groups. The presence of carbonyls groups might be related to the contribution of oxidized low phenolic content in the lignin.

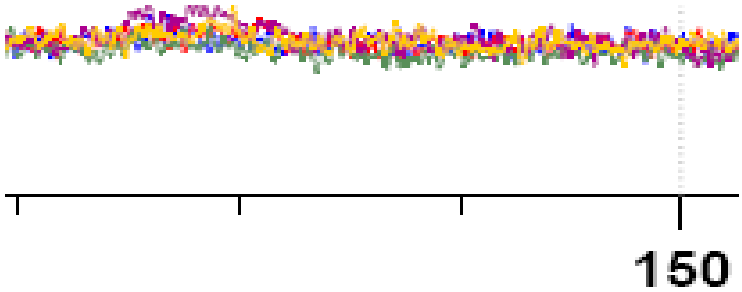

Figure 8: ^{13}C-NMR of displayed spectral superposition (zone :180-150 ppm) of 16th centuries sample after 1,3,7,21 and 28 days of ageing. The marked cellulose deterioration showed after 28-day aged (NMR 4).

As a conclusion after accelerated ageing in a wet environment (1 to 28 days), and on the basis of the ^{13}C NMR data, the aged 28-day sample presents the most degraded chemical structure of the cellulose (oxidized in C=O); and so, reveals that the amorphous phase is the more affected than predominant crystalline form. The ^{13}C NMR finding corroborates with our IR studies and shows that the amorphous form is the most exposed and susceptible to degradation than crystalline one. The same results were obtained and confirmed by Oldak et al. (2005) [45]. The new former are also, responsible together on the new restructuration and reorganization of the polymeric cellulose chain (microfibril structure). Concerning the aged sample (21 days), the structural change affected crystalline and amorphous cellulose form (62-105 ppm) showing a slight deterioration at the wide range of 170-176 ppm.

The solid state ^{13}C NMR results combined to IR finding justify the predominance of resolved crystalline form in cellulose I at the absorptions bands of 1425, 1375 and 1317 cm^{-1} [17-18], while the bands determining the minor resolved amorphous form (cellulose II) are showed with a shape of the broad band in the region of 1500-1400 cm^{-1} , whose most resolved band at 1420 cm^{-1} and the most characteristic of this form , followed by the peak at 1330 cm^{-1}, and the signal at 897 cm^{-1} (*weak* and *broad* band).

In order to assess the state of conservation, the NMR results (a nondestructively tools) provide information on some deterioration processes of aged historical documents (28 days of ageing, under dry-moist weathering effect), discriminate different degrees of paper degradation, and detect the alteration of the crystalline/amorphous cellulose balance (more pronounced with amorphous form). The non-invasive investigation by NMR shows a great promise for future use in damage assessment of cultural heritage documents, contributing to current preservation efforts.

The obtained results lead us to conclude that the addition of 100% of relative humidity in the moist-ageing process is a degradation agent of carbohydrate constituents papers especially cellulose (28 days).
The combination of both spectroscopic techniques ^{13}C NMR/CP-MAS and FTIR seems to be an appropriate tools to establish the change of the molecular structure, introduced by different treatments. The occurrence of oxidation reaction has been confirmed as the main alteration pathway during this process of manuscripts ageing.

Conclusion

The moist-heat weathering treatment induced several modifications in cellulosic matrix of cultural heritage paper mainly for the 16th centuries sample after 28 days of ageing, followed by a slight deterioration after 21 days of ageing; while the dry-heat ageing phenomenon presents no effect during the treatment phases and stills without significant changes, and so, without generation of cellulose oxidation in the restored papers.

The combinations of both spectroscopic techniques, including ^{13}C NMR/CP-MAS and FTIR have shown a good performance, and permit to monitor the induced damages in cellulosic paper with revealing the occurrence of degradation towards the C=O former, and assessing the degree of crystalline/amorphous after prolonged artificial ageing. The obtained results corroborate well and are in complete agreement.

The solid-sate ^{13}C NMR as a non-invasive investigation tools, was used to assess the state of conservation, and reveals that the 16 centuries sample is more exposed to deterioration processes than the others one justified by the oxidized C=O former between 167-176 ppm. The amorphous phase is the more sensitive one to thermal and ageing processes of degradation than predominant crystalline form, and so, is the most affected during extended aged processes (28 days).

The IR as a nondestructively technique, confirms well the NMR results and provides information on caused damage assessment mainly for the 16th centuries after 28 days of ageing moist-heat conditions. The IR results

discriminated the degree of degradation by the presence of new and intense absorption bands correlated to the C=O groups (oxidized cellulose + contribution of extended oxidized lignins content) and permits to distinguish between the crystalline/amorphous cellulose balance, more accented with amorphous form.

Finally, both techniques contribute to current preservation efforts in the field of the state of conservation of the ancient Moroccan manuscripts papers. Based on all obtained results, we could conclude that the restoration process under evaluation did not preserve the papers in the long term. This is an indication that the performance of conservative methods applied in Moroccan libraries should be improved to better preserve the national written cultural heritage.

Acknowledgement

The authors are grateful to Pr Dr. Pierre Doumenq (Aix-Marseille University, France) for recording the FTIR spectrum, and to Dr. M. Kajjout (Lille University, France) for recording the solid state ^{13}C NMR CP/MAS spectra.

References

1. E. Sjostrom, Wood Chemistry. San Diego, CA: Academic Press, Inc., 1981.
2. I. Santoni, E. Callone, A. Sandak, S. Dirè, *Carbohyd. Polym*. 117 (2015) 710-721.
3. L. Hajji, A. Boukir, J. Assouik, H. Lakhiari, A. Kerbal, P. Doumenq, G. Mille, M. L. Carvalho, *Spectrochim. Acta A* 136 (2015) 1038-1046.
   DOI: 10.1016/j.saa.2014.09.127
   http://www.sciencedirect.com/science/article/pii/S1386142514014851
4. D. Tamburini, J. J. Lucejko, M. Zborowska, F. Modugno, E. Cantisani, M. Mamonova, M. P. Colombini, *Int. Biodeter. Biodegr.* 116 (2017) 243-259.
5. K. Kavkler, N. Gunde-Cimerman, P. Zalar, A. Demsar, *Polym. Degrad. Stabil*. 96 (2011) 574-580.
6. L. Hajji, A. Boukir, J. Assouik, S. Pessanha, J. L. Figueirinhas, M. L. Carvalho, *Microchem. J.* 124 (2016) 646-656.
   DOI: **10.1016/j.microc.2015.10.015**
   http://www.sciencedirect.com/science/article/pii/S0026265X15002453
7. J. P. Henk, Rate of Paper Degradation. The Predictive Value of Artificial Aging Tests, European Commission on Preservation and Access, Amsterdam, 2000.
8. A. El Bakkali , T. Lamhasni , M. Haddad , S. Sanchez-Cortes , E. Del Puerto Nevado , *J. Raman Spectrosc*. 44 (1) (2013) 114.
9. A. El Bakkali , T. Lamhasni , S. Ait Lyazidi , S. Sánchez-Cortés , M. El Rhaiti , *Vib. Spectrosc*. 74 (2014) 47.
10. L. Hajji, A. Boukir, J. Assouik, A. Kerbal, M. Kajjout, P. Doumenq, M. L. Carvalho, *Appl. Spectrosc.* 69 (8) (2015) 920-938.
    DOI: 10.1366/14-07688
    http://asp.sagepub.com/content/69/8/920
11. L. Cabrales, N. Abidi, A. Hammond, A. Hamood, *J. Mater. Environ. Sci.* 3 (3) (2012) 561-574.
12. K. Azzaoui, E. Mejdoubi, A. Lamhamdi, S. Zaoui, M. Berrabah, A. Elidrissi, B. Hammouti, M.G. Fouda Moustafa, S. S. Al-Deyab, *Carbohyd. Polym*. 115 (22) (2015) 170-176.
    DOI: 10.1016/j.carbpol.2014.08.089
13. M. Bardet, M.F. Foray, Q.-K. Tran, *Anal. Chem.* 74 (2002) 4386-4390.
14. S. Bastone, A. Spinella, D. F. Chillura Martino, S. Tusa, E. Caponetti, *Microchem. J.* 124 (2016) 831-836.
15. M. Traoré, J. Kaal, A. M. Cortizas, *Spectrochim. Acta A* 153 (2016) 63-70.
16. J.-B. Chen, Q. Zhou, S.-Q. Sun, *J. Mol. Struct*. 115 (2016) 55-62.
17. N. Abidi, L. Cabrales, C. H. Haigler, *Carbohyd. Polym*. 100 (2014) 9-16.
18. S. Acharya, Y. Hu, H. Moussa, N. Abidi, *J. Appl. Polym. Sci.* 134 (21) (2017).
19. S. Durmaz, O. Ozgenc, I. H. Boyaci, U. C. E. Yildiz, Erisir, *Vib. Spectrosc*. 85 (2016) 202-207.
20. Y. Maréchal, H. Chanzy, *J. Mol. Struct*. 523 (2000) 183-196.
21. P. Garside, P. Wyeth, *Stud. Conserv*. 48 (2003) 269-275.
22. Y. Song, J. Zhang; X. Zhang, T. Tan, *Bioresource Technol*. 193 (2015) 164-170.
23. R.H. Atalla, D.L. Vanderhart, *Science*. 223(4633) (1984) 283-285.
24. M. Paci, C. Federici, D. Capitani, N. Perenze, A.L. Segre, *Carbohyd. Polym*. 26 (1995) 289-297.
25. M. Foston, *Curr. Opin. Biotech.*, 27 (2014) 176-184.
26. H. Kono, C. Oka, R. Kishimoto, S. Fujita, *Carbohyd. Polym*. 170 (15) (2017) 23-32.
27. L. Segal, J.J. Creely, A.E. Jr. Martin, C.M. Conrad, *Text. Res. J.* 29 (10) (1959) 786-794.

28. S. Nam, A. D. French, B. D. Condon, M. Concha, *Carbohyd. Polym*. 135 (2016) 1-9.
29. M. Poletto, A. J. Zattera, A. C. Forte, R.M.C. Santana, *Bioresource Technol*. 109 (2012) 148-153.
30. M.L. Carvalho, C. Casaca, T. Pinheiro, J.P. Marques, P. Chevallier, A.S. Cunha, *Nucl. Instrum. Methods Phys. Res., Sect. B*. 168 (2000) 559-565.
31; M. Schwanninger, J.C. Rodrigues, H. Pereira, B. Hinterstoisser, *Vib. Spectrosc*. 36 (2004) 23-40. http://dx.doi.org/10.1016/j.vibspec.2004.02.003 http://www.sciencedirect.com/science/article/pii/S092420310400030X
32. P. Calvini, A. Gorassini, *Restaurator* 23 (2002) 48-66.
33. A. Boukir, E. Aries, M. Guiliano, L. Asia, P. Doumenq, G. Mille, *Chemosphere* 43 (3) (2001) 279-286. **DOI:** 10.1016/S0045-6535(00)00159-4 http://www.sciencedirect.com/science/article/pii/S0045653500001594
34. A. Boukir, M. Guiliano, P. Doumenq, G. Mille, *C. R. Acad. Sci. – Series IIC – Chemistry* 1 (10) (1998) 597-602. DOI:10.1016/S1387-1609(99)80013-9 http://www.sciencedirect.com/science/article/pii/S1387160999800139
35. C. Invernizi, A. Daveri, T. Rovetta, M. Vagnin, M. Licchelli, *Microchem. J.* 124 (2016) 743-750.
36. B. Zghari, P. Doumenq, A. Romane, A. Boukir, *J. Mater. Environ. Sci.* 8(12) (2017) 4496-4509.
37. SY. Oh, DI. Yoo, Y. Shin, G. Seo, *Carbohyd. Res*. 340 (2005) 417-28.
38. LM. Proniewicz, C. Paluszkiewicz, A. Weselucha-Birczynska, H. Majcherczyk, A. Baranski, A. Konieczna, *J. Mol. Struct*. 596 (2001) 163-9.
39. KK. Pandey, T. Vuorinen, *Polym. Degrad. Stabil.* 39 (12) (2008) 2138-46.
40. A. Xu, L. Cao, B. Wang, *Carbohyd. Polym*. 125 (2015) 249-254.
41. N.B. Colthup, L. H. Daly, S.E. Wiberley, In: Introduction to Infrared spectroscopy and Raman spectroscopy, second ed. Academic Press, New York, 1975.
42. D. L. Pavia, G. M. Lampman, G. S. Kriz, Introduction to Spectroscopy. A Guide for Students of Organic Chemistry, 2nd Edition, Saunders Golden Sunburst Series, 1996, pp. 67-68.
43. O. Faix, *Holzforschung* 45 (1991) 21-28.
44. X. Colom, F. Carrillo, *Eur. Polym. J*. 38 (2002) 2225-2230.
45. D. Oldak, H. Kaczmarek, T. Buffeteau, C. Sourisseau, *J. Mater. Sci*. 40 (16) (2005) 4189-98.

(2018) ; http://www.jmaterenvironsci.com